Optical Probing of Laser Induced Plasma

H. Waheed[1,2*], K. A. Bhatti[1] and S. Ashraf[1,2]
[1]*Laser and Optronics Center, Department of Physics, University of Engineering and Technology, Lahore, Pakistan*
[2]*Department of Physics, University of Management and Technology, Lahore, Pakistan*

An investigation on the phenomenon of plume dynamics is undertaken experimentally as well as theoretically. A Q-switched Nd: YAG laser (1064 nm, 10 mJ, 1.1 MW, 9-14 ns) is tightly focused on different target metals, carbon and EPDM samples (2cm x 2cm x 0.2 cm) at an angle of 45^o with the normal of the target surfaces. The experiments were performed in air at standard temperature and pressure (298K and 760 Torr pressure). CW He-Ne laser (633 nm) employed a probe beam for plasma plume investigation. CCD based computer controlled image capturing system was used to store images on the computer system. The shadows show changes in various parameters as time elapsed after production of material ablation. Shock wave and Drag models have been applied to draw the experimental data. The results thus obtained show different density regimes of the plasma along with the shock waves. The plume expansion exhibits a linear expansion of plume at earlier times, but at later times, plasma plume expansion becomes non-uniform and plume becomes spherical. There is a bright nucleus at the center at earlier times that vanishes at later times. Shock wave detaches itself at later times.

1. Introduction

Laser-matter interaction and laser induced plasma (LIP) is a growing field of interest for scientists and engineers due to its vast applications [1-4]. During laser-matter interaction, laser energy is absorbed by the target material to cause laser induced plasma. Thus electromagnetic energy is converted into electronic excitation, then into thermal, chemical and mechanical energy in order to cause melting, evaporation, ablation processes [5]. The ablated material continues to absorb heat until a stage reaches when plasma formation occurs. Laser induced plasma plume is a cloud of ejected material having ions, electrons and neutrals [1]. Plasma plume starts expanding and its expansion in ambient gas is affected by the background atoms and molecules [6]. Its expansion is determined by the interaction of plume atoms with the background atoms and molecules [1]. Plume expansion in ambient gas medium undergoes many processes like deceleration, attenuation, thermalization, formation of shock waves, and many other [7,8]. Thus it is very important to investigate plume dynamics.

Several diagnostic techniques have been proposed for the plume dynamics, like fast photography [9,10], spectroscopy [10,11], and shadow-graphy [12-17].

In order to employ optical probing technique it should fulfill some conditions e.g., light source must be of small dimensions and brightness should be sufficient in order to overcome intense plasma radiation. As it depends on wavelength of incident radiation so mono-chromaticity is desirable. This technique is based on the refraction of electromagnetic waves and electron density, so it depends on the second gradient of the refractive index [12,13].

Optical probing of plasma plume is a useful technique and is used to study the fluid and gas dynamics. This technique is beneficial in aeronautical science and engineering. It is also used to study shock wave phenomenon.

2. Models on Plasma Expansion Dynamics

Plasma expansion dynamics have been investigated theoretically as well experimentally. Several models have been proposed for the plume dynamics. Some of them are described in the sequel.

2.1. Shock wave model

The shock wave model is employed for earlier times of the plume dynamics in the background gas when plume expansion is isothermal. The expansion of shock wave model from Taylor-Sedov theory is given [18-22] as

*hafsa.waheed@umt.edu.pk

$$R(t) = \xi_0 \left(\frac{E}{\rho}\right)^{\frac{1}{5}} t^{2/5} \quad (1)$$

Where, ξ_0 is a constant that depends on specific heats of background gas and plasma, 'R' is the distance covered by shock wave, 'E' is the explosion energy released by shock wave, ρ is the gas density and 't' is the delay time. If some initial time t_0 is given then the expansion of shock wave is given by following expression [21].

$$R(t) = \xi_0 \left(\frac{E}{\rho}\right)^{\frac{1}{5}} (t - t_0)^{2/5} \quad (2)$$

Where, 'R' is shockwave displacement, t is the delay time and t_0 is the initial time.

Shock wave model is employed at higher background pressure. A strong shock wave is formed at the front boundary that pushes the background gas like some piston exerting pressure on it due to a sudden release of explosion energy [19-22].

2.2. Drag model

Drag model is applied to plume dynamics at later times when plume starts expanding adiabatically. The ablated mass acting as an ensemble of particles will experience a viscous drag force when passing through the background gas [19,20]. So drag model is given by the equation [20-22]

$$x = x_{max}[1 - e^{\beta t}] \quad (3)$$

Where, x_{max} is the maximum distance covered by the plume, while β is the slowing coefficient.

3. Experimental Setup

Nd:YAG laser (1064 nm,10 mJ,1.1 MW, 9-14 ns) is tightly focused on the target materials (C, Al, Cu, Fe, Ag, EPDM) to generate plasma. In order to probe the dynamics of plume CW He-Ne laser (633 nm) is passed through the plasma. Probe laser is expanded and collimated with the help of an assembly of concave and convex lenses of different focal lengths. The defocused (magnified) images are captured by CCD based computer controlled image grabbing system, which are stored on personal computer for analysis.

4. Results and Discussion

The images show a dense core region indicating plasma plume, while the outer region contains two shockwaves. One is a primary/external shock wave SW_1, which moves with the supersonic speed initially and is formed due to the sudden pressure exerted by the excited plume atoms and molecules on background gas. The propelling atoms are excited, that results in the increase of thermal energy, thus leading to the formation of secondary/internal shock wave SW_2 inside plasma [8, 23-25]. The plume and both primary and secondary shockwaves increase with time, but then their propagation slow down and become almost constant with increasing time.

From Fig. 1(a,b,c), it is observed that displacement against time graphs show an exponential increase with time. It is shown from that for a long time shockwave from EPDM propagated upto larger displacement than any other targets, and shock wave remains for longer time than the other target.

As it is clear from the Fig. 1(a), the displacement covered by primary shock wave d_{SW1} goes up to 13.53 mm upto 300000 ns, while for any other target the time delay is taken upto the 8000 ns. Shockwave formation by silver and carbon travels almost same displacements, though shockwave in silver it iniates earlier; d_{SW1} for the silver initiates from 4.12 mm and for carbon it is from 5.15 mm, but for carbon and silver d_{SW1} ends at 6.06 mm and 6.13 mm. Shockwave formed by aluminum plasma propagates to more displacement than carbon and silver; maximum d_{SW1} for aluminum is 8.80 mm.

The same behavior is shown in Fig. 1(b) for the displacement covered by secondary shock wave d_{SW2} for aluminum propagates more than carbon and silver and EPDM has the highest d_{SW2}. The maximum d_{SW2} for EPDM is 12.40 mm, whereas for carbon d_{SW2} is 5.62 mm, for d_{SW2} silver it is 5.56 mm and for aluminum d_{SW2} is 7.89 mm.

Similarly, the plume expansion d_{plume} for the polymer is higher than other targets as shown in Fig. 1(c). And for aluminum it is more than carbon and silver. While for carbon and silver plume front position d_{plume} is almost the same. Maximum dispalcement for the plume front poisition for carbon is 2.40 mm, for silver it is 2.78 mm, for aluminum d_{plume} is 4.63 mm, and for EPDM it is 9.03 mm.

The velocity versus time graphs for all the material targets show an exponential decrease with time for all the target materials. From the comaprison graphs in Fig. 3(a,b,c) it is observed that the polymer has the lowest velocity while aluminum shows the highest velocity in all the three graphs of comparison.

In Fig. 2(a), the maximum velocity of primary shockwave v_{SW1} for aluminum is 1.45×10^5 m/s and it goes down to the value of 1.11×10^3 m/s. Similarly for the carbon v_{SW1} starts from 1.03×10^5 m/s down to 7.66×10^2 m/s, whereas for silver it moves from 4.12×10^4 m/s down to 7.57×10^2 m/s, which shows that both carbon and silver exhibits the same final values of shockwave velocities. For EPDM, v_{SW1} initiates from1.21×10^4 m/s to 45.11 m/s, thus having the lowest value of shockwave velocity.

Figure 2(b) shows the same trend as in the previous figure, alumiunum exhibits highest values of velocity of secondary shockwave v_{SW2}, while EPDM shows the lowest. The maximum velocity v_{SW2} for aluminum is 1.33×10^5m/s and it goes down to the value of 9.8×10^3 m/s. Similarly for the carbon v_{SW2} starts from the 9.4×10^4 m/s and goes down to 6.95×10^2 m/s, while for silver it moves from6.70×10^4 m/s down to 7.02×10^2 m/s, which again shows that both carbon and silver exhibits the same final values of shockwave velocities. For the EPDM, v_{SW2} initiates from 1.12×10^4 m/s to 41.32 m/s, thus having the lowest value of shockwave velocity.

The same behavior of velocities is shown for the plume expansion in Fig. 2(c). Aluminum plume moves with higher velocities than the other target materials, and polymer has the lowest one. The maximum plume velocity v_{plume} for aluminum is 8.03×10^4 m/s and it goes down to the value of 5.79×10^2 m/s. Similarly for the carbon v_{plume} starts from the 4.23×10^4 m/sdown to 2.99×10^2 m/s while for silver it moves from 6.83×10^4 m/s down to 3.47 $\times10^2$ m/s. And for the EPDM, v_{plume} initiates from 8.16×10^3 m/s to 30.11 m/s, thus having the lowest value of plume velocity.

The graphical representation for the acceleration versus time for all the targets show an exponential decrease with time as shown in Fig. 3(a,b,c). From the graphical representation, it is clear that aluminum has the highest acceleration in comparison with the other targets. While EPDM shows the lowest value of acceleration.

From Fig. 3(a), primary shockwave accelaration a_{SW1} of aluminum initiates from 8.87×10^2 m/s^2 and ends at 0.14 m/s^2, thus having the highest shockwave acceleration, and $a_{SW1}$for carbon and silver have almost same final values of acceleration i.e., a_{SW1} for carbon has value of 6.7×10^2 m/s^2 to 0.094 m/s^2, while for a_{SW1} of silver starts from 5.49×10^2 m/s^2 to 0.095 m/s^2. And EPDM possess lowest value of shockwave acceleration, i.e., for polymer a_{SW1} starts from 3.75 m/s^2 to 2×10^{-3} m/s^2.

Figure 3(b) presents the same trend for the secondary shockwave accelaration as for the previous one, i.e., a_{SW2} of aluminum possess highest value, initiates from 8.55×10^2 m/s^{2}and ends at 0.12 m/s^2, thus having the highest shockwave acceleration; a_{SW2} for carbon and silver have almost same final values of acceleration i.e., a_{SW2} for carbon has value of 6.20×10^2 m/s^2 to 0.087 m/s^2, while for a_{SW2} of silver starts from3.88×10^2 m/s^2 to 0.088 m/s^2. EPDM possess the lowest value of shockwave acceleration, i.e., for polymer a_{SW2} starts from3.40 m/s^2 to 10^{-3} m/s^2.

The plume expansion acceleration as shown in Fig. 3(c) also exhibits the same behavior as for the shockwave acceleration. Aluminum has highest value plume acceleration i.e., a_{SW2} for aluminum starts from 6.17×10^2 m/s^2 and ends at 0.072 m/s^2. Similarly a_{plume} for carbon and silver have almost same final values of plume acceleration i.e., a_{plume} for carbon has value of 2.95×10^2 m/s^2 to 0.037 m/s^2, while for a_{plume} of silver starts from 5.32×10^2 m/s^2 to 0.043 m/s^2. And EPDM possess lowest value of shockwave acceleration, i.e., for EPDM a_{plume} starts from 2.29 m/s^2 to 10^{-3} m/s^2.

5. Conclusions

Plasma is transient in nature and it shows different regimes. Different facts like deceleration, snowplowing effect and formation of shockwaves are also prominent. The displacement for primary and secondary shock waves and the plume increase with an increase in time, which shows a linear relation as in Fig. 1 [26-30]. So the displacement covered by primary and secondary shockwaves $d_{SW1}$and $d_{SW2,}$ as well as for the plume d_{plume} are 13.53 mm, 12.40 mm and 9.03 mm, respectively, at 3×10^5 ns as in Fig. 1. While the velocity and acceleration for the shockwave and plume decrease with an increase in time. Velocity for the primary and secondary shockwaves v_{SW1} and $v_{SW2\ ,}$as well as for the plume v_{plume} show a decrease in values i.e., 45.11 m/s, 41.21 m/s and 30.11 m/s, respectively, at 3×10^5 ns as in Fig. 2. Values of acceleration for primary and secondary shockwaves $a_{SW1}$and $a_{SW2,}$ as well as for the plume, a_{plume} show a decrease in values i.e., 2×10^{-3} m/s^2, 10^{-3} m/s^2 and 10^{-3} m/s^2 , respectively, at 3×10^5 ns as shown in Fig. 3.

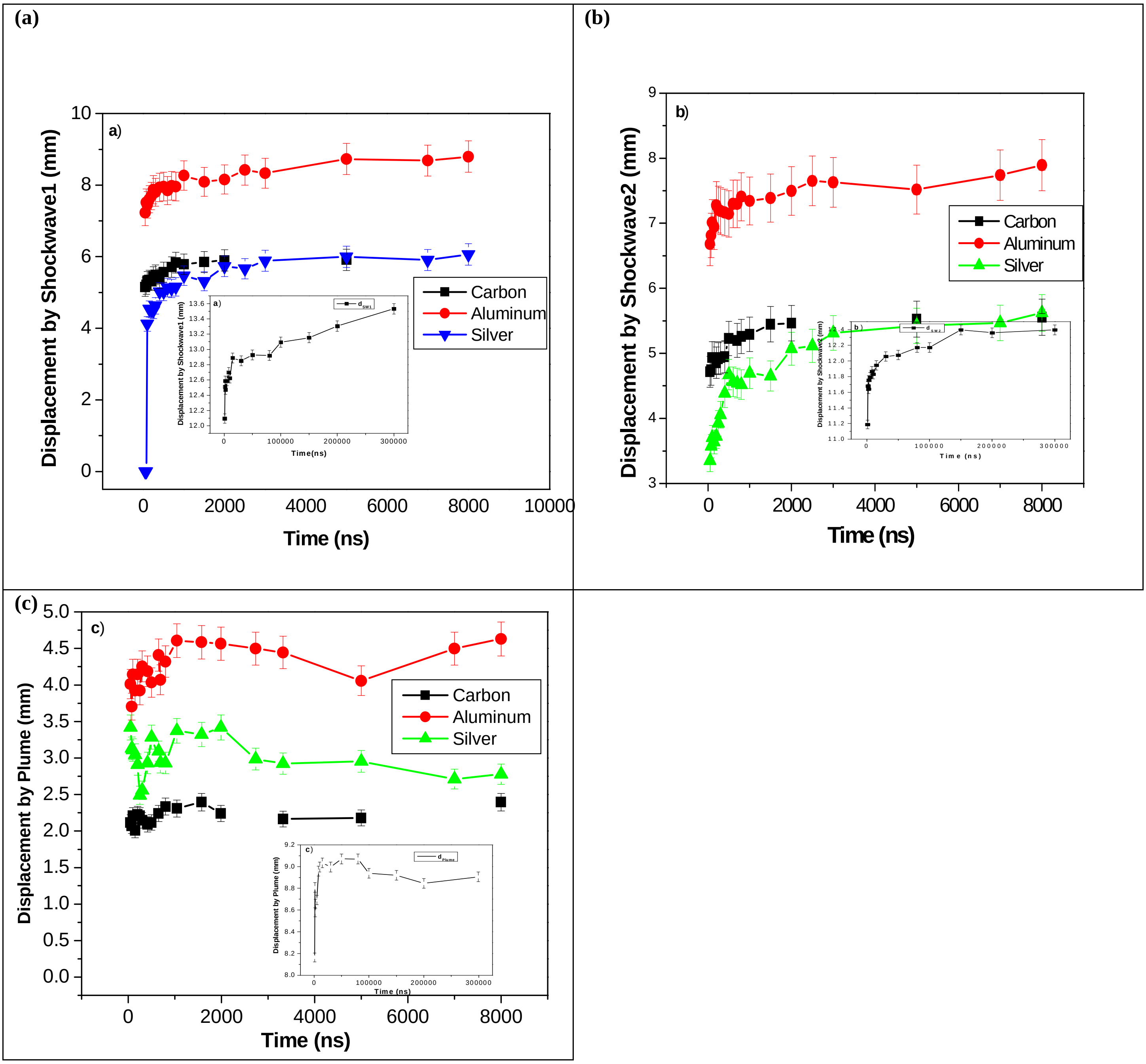

Fig.1: Displacement versus time graph for different material plume for (a) Shockwave1 (d_{SW1}) (b) Shockwave2 (d_{SW2}) and (c) Plume front (d_{plume})

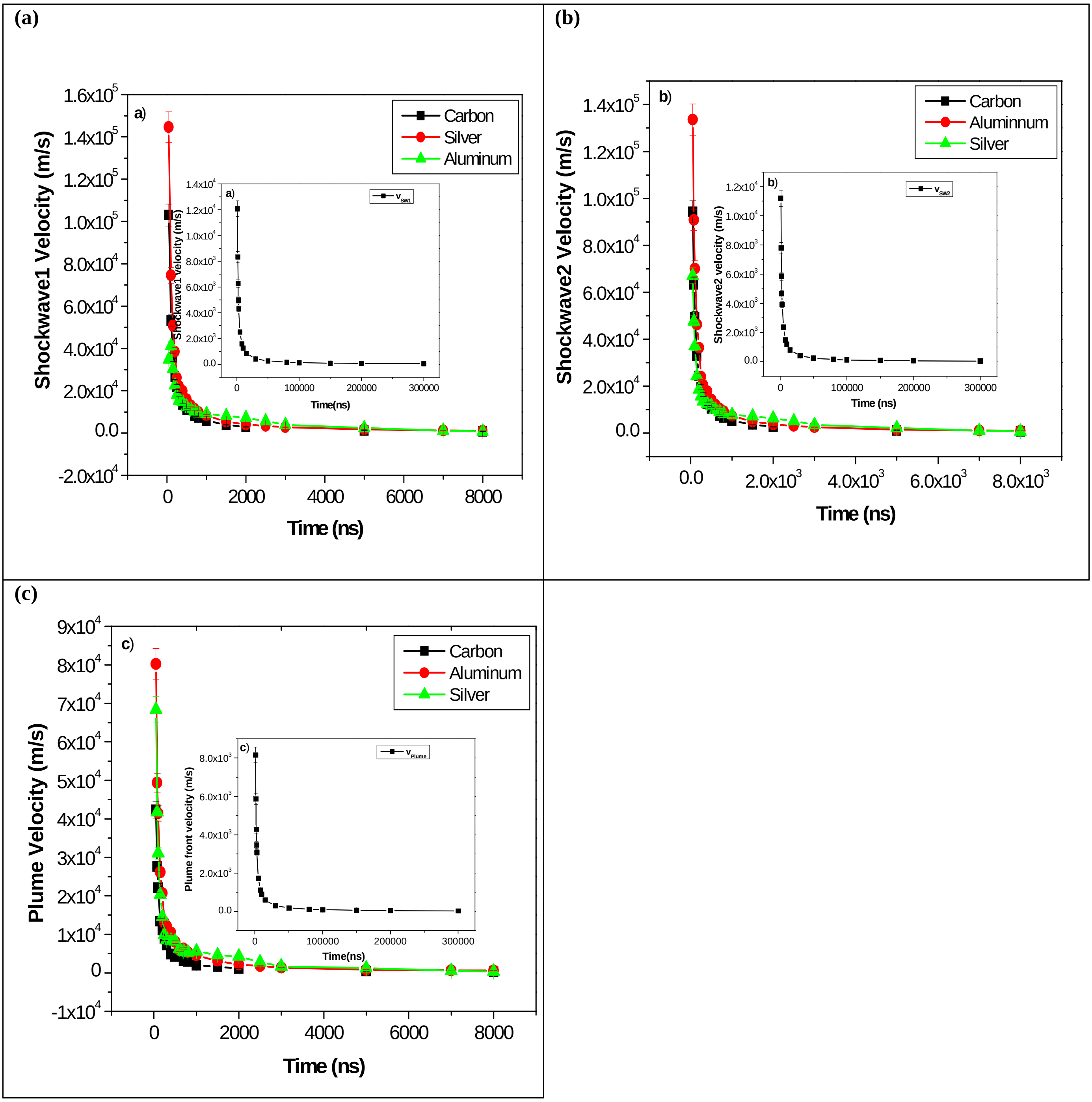

Fig.2: Velocity versus time graphs for different material plume for (a) Shockwave 1 (v_{SW1}) (b) Shockwave 2 (v_{SW2}) and (c) Plume front (v_{plume})

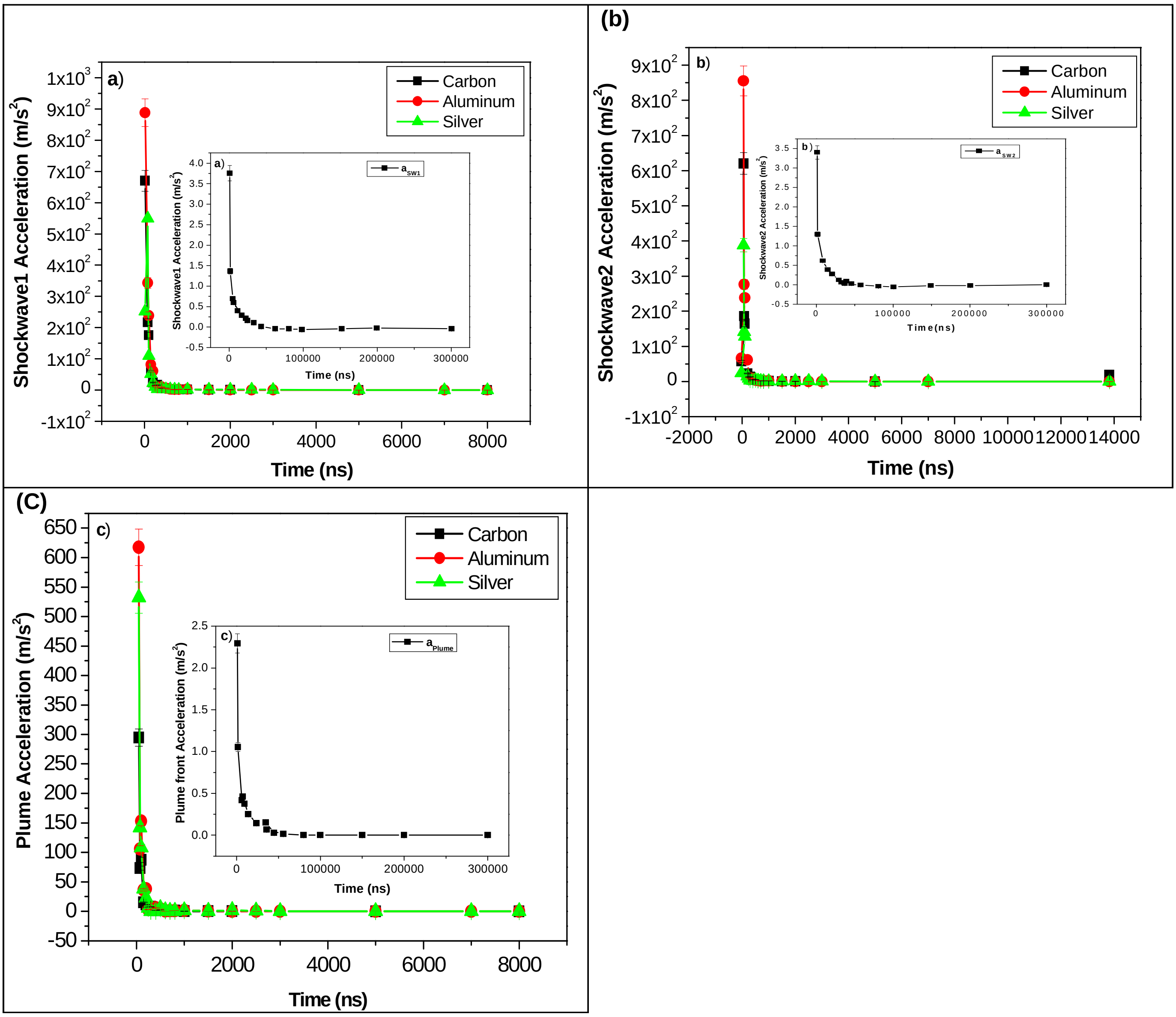

Fig.3: Acceleration versus time graphs for different material plume for (a) Shockwave1 (a_{SW1}) (b) Shockwave 2 (a_{SW2}) and (c) Plume front (a_{plume})

References

[1] Claude R. Phipps, *Laser Ablation and Its Application* (Springer Link, New York, USA, 2007).

[2] Leon J. Radziemski and David A. Cremers, *Laser Induced Plasma and Applications* (Marcel Dekker Inc., 270 Madison Avenue, New York, 1989).

[3] Suresh Kumar, PhD. Thesis, NSSE, NIE, NTU, Singapore (1996).

[4] K. A. Bhatti, M. S. Rafique, M. Khaleeq-ur-Rahman, A. Latif, K. Hussain, A. Hussain, K. T. Chaudhary, B. A. Tahir and R. Qindeel, Vacuum **85**, 915 (2011).

[5] D. B. Chrisey and G. K. Hubler, (Eds.), *Pulsed Laser Deposition of Thin Films* (Wiley, New York, 1994).

[6] F. Garrelie, C. Champeaux and A. Catherinot, Applied Physics A **69**, S55 (1999).

[7] A. V. Bulgakov and N. M. Bulgakova, J. Phys. D: Appl. Phys. **28**, 1710 (1995).

[8] A. V. Bulgakov and N. M. Bulgakova, J. Phys. D: Appl. Phys. **31**, 693 (1998).

[9] S. S. Harilal, B. O'Shay, M. S. Tillack, C. V. Bindhu and F. Najmabadi, Plasma Science **33**, 474 (2005).

[10] S. S. Harilal, C. V. Bindhu, M. S. Tillack, F. Najmabadi and A. C. Gaeris, J. Phys. D: Appl. Phys. **35**, 2935 (2002).

[11] S. S. Harilal, C. V. Bindhu, V. P. N. Nampoori and C. P. G. Vallabhanb, Appl. Phys. Lett. **72**, 167 (1998).

[12] Wang Wei Long PhD Thesis, NSSE, NIE, NTU, Singapore (2000).

[13] Richard H. Huddlestone and Stanley L. Leonard, *Plasma Diagnostic Techniques* (Academic Press, New York, 1965).

[14] William Whitty and Jean-Paul Mosnier, Appl. Surf. Sci. **127–129**, 1035 (1998).

[15] D. Breitling, H. Schittenhelm, P. Berger, F. Dausinger and H. Hügel, Appl. Phys. A **69**, S505 (1999).

[16] F. Kokai, K. Takahashi, K. Shimizu, M. Yudasaka and S. Iijima, Appl. Phys. A **69**, S223 (1999).

[17] K. A. Bhatti, PhD. Thesis, Department of Physics, UET Lahore (2010).

[18] P. Lee, S. Kumar and S. Lee, Laser and Particle Beams **16**, 317 (1998).

[19] S. Mahmood, R. S. Rawat, M. Zakaullah, J. J. Lin, S. V. Springham, T. L. Tan and P. Lee, J. Phys. D: Applied Physics **42**, 1 (2009).

[20] David B. Geohegen, Appl. Phys. Lett. **60**, 2732 (1992).

[21] S. Lafane, T. Kerdja, S. Abdelli-Messaci, S. Malek and M. Maaza, Appl. Phys. A **98**, 375(2010).

[22] Wee-OngSiew, Teck-Yong Tou, Seong-Shan Yap, Kah-Hieng Wong and Oi-Hoong Chin, Plasma Science **31**, 1299 (2003).

[23] G. Cristoforetti, S. Legnaioli, L. Pardini, V. Palleschi, A. Salvetti and E. Tognoni, SpectrochimicaActa Part B **61**, 340 (2006).

[24] A. M. Marpaung, R. Hedwig, M. Pardede, T. J. Lie, M. O. Tjia, K. Kagawa and H. Kurniawan, SpectrochimicaActa Part B **55**, 1591 (2000).

[25] J. P. Chen, X. W. Ni, J. Lu and B. M. Bian, Optics Communications **176**, 437 (2000).

[26] G. Settles, *Schlieren and Shadowgraph Techniques, Visualizing Phenomena in Transparent Media* (Springer-Verlag, Berlin, New York, 2001).

[27] Mohammad Hendijanifard and David A. Willis, Proceedings of HT2009 ASME Summer Heat Transfer Conference, San Francisco, California, USA (2009).

[28] Tsuyoshi Noguchi and KunihitoNagayama, Diamond and Related Materials **12**, 953 (2003).

[29] V. V. Osipov, V. V. Platonov and V. V. Lisenkov, Quantum Electronics **39**, 541 (2009).

[30] M. Hauer, D. J. Funk, T. Lippert and A. Wokaun, Optics and Lasers in Engineering, **43**, 545 (2005).

Received: 17 June, 2016
Accepted: 10 October, 2016